Performance Analysis of sub-6 GHz/mmWave NOMA Hybrid-HetNets using Partial CSI

Performance Analysis of sub-6 GHz/mmWave NOMA Hybrid-HetNets using Partial CSI

Pragya Swami, Mukesh Kumar Mishra, Vimal Bhatia, *Senior Member, IEEE*, Tharmalingam Ratnarajah, *Senior Member, IEEE*, and Aditya Trivedi, *Senior Member, IEEE*

***Abstract*—The ever-increasing number of wireless users (or devices) and their varied demand require the need for an advanced architecture for the future wireless network. To support massive connectivity, non-orthogonal multiple access (NOMA) has been recognized as a promising solution. NOMA increases the number of simultaneous connections using available resources for users with varying demands. Furthermore, recent measurements and experiments suggest that wide underutilized bandwidth available at millimeter-wave (mmWave) frequencies provide high data rate and therefore are capable of addressing the issue of spectrum scarcity at sub-6 GHz bands utilized by the 4G network. Consequently, co-existence of multi-radio access technologies (RATs) for 5G and beyond networks has been of interest to both industries and academia. In this context, this work studies the co-existence of the two RATs, namely, sub-6 GHz and mmWave communication using NOMA-enabled hybrid heterogeneous network (NOMA-HHN) for massive connectivity. The application of NOMA requires ordering users, which in turn requires the knowledge of users' channel state information (CSI). However, gathering and processing CSI of such a large number of users is difficult to implement in practice. Thus, a solution based on partial CSI is proposed. Additionally, a feedback scheme for user scheduling and RAT selection using dual association is proposed to reduce the initial access delay in beam-training at the mmWave network. Moreover, utilizing directional nature of the mmWave communication, random beamforming is used to reduce system overhead in a network with massive users. The analytical results are confirmed using Monte-Carlo simulation, and various significant advantages are noted for the proposed NOMA-HHN over existing architectures.**

***Index Terms*—Non-orthogonal multiple access, mmWave communication, hybrid network, partial CSI, outage probability, ergodic rate, energy efficiency**

I. Introduction

The current research considers non-orthogonal multiple access (NOMA) as a promising technique for the beyond fifth-generation (5G) networks to fulfill diverse demands and massive number of users (or devices). As the number of users increases, assigning orthogonal resources to all the users is not feasible due to restricted resources. Furthermore, allocating an entire band or time slot to a user with poor channel condition or with lower rate requirement leads to wastage of precious and expensive resources, thereby resulting in poor spectral efficiency. NOMA allows multiple users to be served on the same wireless resource, hence improves spectral efficiency of the system and scales up the number of connected users (or devices). NOMA can be flexibly combined with other emerging technologies, for instance, heterogeneous networks (HetNet) [1], [2] millimeter wave (mmWave) communication [3], [4], [5], and others [6]–[9]. Densification of the current cellular networks can be achieved by deploying small base stations (SBSs) underlaid with the macro base stations (MBSs) to form a HetNet, which is an essential part of the beyond 5G communication system [10]. The deployment of SBSs aids in offloading users from the MBS tier, thereby resulting in load balancing in the network. It is known that mmWave communication can significantly boost achievable data rates using the available large underutilized channels [3]. However, imagining a standalone wireless network with base stations (BSs) supporting only mmWave band is not a practical approach in 5G for ubiquitous connectivity, since mmWave channels suffer from substantial attenuation and high sensitivity to blockages [4], [11]. In addition, providing initial access to standalone mmWave BS using beam training with thin beams poses a difficult challenge [3], [12]. In this regard, the sub-6 GHz band can be used to aid the initial access mechanism [13]. If the position of the sub-6 GHz-SBS and the mmWave-SBS are known relative to each other, information required for beam training at the mmWave front-end can be derived easily, which consequently speeds up the initial access mechanism [14], [13]. This indicates that the mmWave communication, in conjunction with sub-6 GHz communication, can be viewed as a promising solution to solve the issues of spectrum scarcity in sub-6 GHz bands and beam training for mmWave communication [15]. Hence, this work investigates NOMA based hybrid HetNet (hereafter referred to as NOMA-HHN), which includes SBS tier equipped with two radio access technologies (RATs), namely, sub-6 GHz communication and mmWave communication.

The SBS tier employs NOMA to support increasing number of users. The available NOMA techniques can be broadly categorized as power-domain NOMA (PD-NOMA) and code-domain NOMA (CD-NOMA) [16], [17], [18]. However, PD-NOMA has a simpler implementation and is thereby com-

This work is supported in part by the R&D work undertaken project under the Visvesvaraya PhD Scheme of Ministry of Electronics and Information Technology, Government of India, being implemented by Digital India Corporation (Grant number 13(28)/2020-CC&BT), and in part by IIT Indore. This work of T. Ratnarajah is also supported by the U.K. Engineering and Physical Sciences Research Council (EPSRC) under Grant EP/P009549/1. This work is also partially supported by the University of Hradec Kralove, Faculty of Informatics and Management, Czech Republic under Grant UHK-FIM-SPEV-2022-2102. We are also grateful for the support of PhD student Michal Dobrovolny for consultations. (Corresponding author: Pragya Swami.)

P. Swami is with the Department of Electronics and Communication Engineering, Pandit Deendayal Energy University, Gandhinagar; Vimal Bhatia is with the Department of Electrical Engineering, Center for Advanced Electronics, Indian Institute of Technology Indore, Indore 453552, India, and also with the Faculty of Informatics and Management, University of Hradec Kralove, 50003 Hradec Kralove, Czech Republic; M. K. Mishra is with Indian Institute of Information Technology Dharwad, India; T. Ratnarajah is with the Institute for Digital Communications, University of Edinburgh, Edinburgh, UK, and Aditya Trivedi is with ABV-Indian Institute of Information Technology and Management Gwalior, India

monly used [17]. Therefore, this work also focuses on PD-NOMA. The basic concept of PD-NOMA (hereafter will be referred to as NOMA) involves splitting the power among the users based on their channel gain [19], [20]. As the capacity of the wireless system increases, a large number of mobile users are likely to be connected to the BS. At the receiver, NOMA requires ordering users based on channel conditions for power splitting, whereas at the receiver successive interference cancellation (SIC) is used at the near user to cancel the interference from the superimposed signal [19]. Both, power splitting and SIC require channel state information (CSI) to be known at the BS and at the user equipment. Collecting CSI from such a large and increasing number of users is difficult [21], however, the current research works mainly focus on the perfect CSI in NOMA systems [22], [23], [24]. Imperfect/partial CSI at the BS and user equipment is still an open problem since it is one of the key obstacles in realizing performance gain of NOMA in practice. Furthermore, due to the directional nature of mmWave communication, random beamforming is a good choice for scheduling users for the proposed NOMA-HHN [25], [26]. The traditional beamforming techniques require channel gains of all the users. However, random beamforming does not require users with low signal strength on the beam to feed their channel gain to the BS. Thus, in a network with massive number of users, mmWave communication using random beamforming reduces the system overhead [25], [26] by scheduling the users with high signal strength on only the beam.

A. Motivation and Contribution

Motivated by the availability of huge chunks of under-utilized mmWave bands, this work studies the co-existence of mmWave communication with sub-6 GHz communication to solve the spectrum crunch with ubiquitous connectivity. Moreover, the advantage of NOMA over orthogonal multiple access (OMA) to support large number of connections with diverse requirements, and the usefulness of offloading in HetNets for load balancing, motivates us to investigate performance of the proposed NOMA-HHN. The analysis is performed under a realistic scenario using partial CSI and is also compared with the conventional (ideal) assumption of perfect CSI at the BS. Utilizing the directional nature of mmWave communication, random beamforming is used to limit the system overhead by scheduling the users with high signal strength on a beam. Furthermore, to address the issue of beam training in mmWave-SBS, this work introduces a feedback scheme using dual association, which facilitates beam training at the mmWave-SBS. Impact of the considered partial CSI and the proposed feedback scheme are investigated on performance of the proposed NOMA-HHN. Various partial CSI models considered in this work are given below:

- Users' distance information (UDI): The complete CSI comprises of small-scale Rayleigh fading and large-scale path loss. UDI implies that knowledge of the large-scale path loss is available, i.e., distances of users from the BS are known. Since, distance varies much slower than the channel in small-scale fading environments [21], assuming knowledge of UDI is more realistic.
- Feedback: In general, the channel is estimated by the user device and transmitted to the BS [27], [28]. Therefore, one practical approach to be considered is feeding back a single bit by the user instead of the complete CSI to the BS. User sends a single bit about the quality of its channel quality indicator [29] which substantially lowers the system overhead. The bit transmitted by the user is determined based on a pre-defined threshold (ζ) broadcasted by the BS. The proposed feedback scheme (FS) using dual association (DA) is based on one-bit feedback and is detailed in Section III.
- No feedback: To show advantage of using feedback, this work also considers the case when neither CSI nor feedback is available at the BS. Under such circumstances, the BS randomly orders the users [28], which results in ambiguous decoding order for the SIC at the user equipment/receiver. Note that NOMA without feedback is a special case of the NOMA with one-bit feedback when the threshold is set as $\zeta = 0$ or $\zeta = \infty$.

Primarily, the contributions of this work are listed below:

- An analytical framework is developed to investigate the impact of mmWave communication, in conjunction with the sub-6 GHz communication on the proposed NOMA-HHN using random beamforming for mmWave communication. In this context, outage probabilities for the proposed NOMA-HHN are derived. For load balancing, two types of offloading are taken into account, one is between the MBS tier and the SBS tier, and the other is between the two RATs supported by the SBS tier. Accordingly, two probabilities are calculated, namely, the tier selection probability and the RAT selection probability. Furthermore, performance of the proposed NOMA-HHN is analyzed, and compared with OMA enabled HetNets and NOMA enabled single-RAT HetNet.
- By virtue of its application, BSs using NOMA require CSI to order users for SIC and power allocation. However, determining the CSI of massive number of users is challenging. Therefore, to tackle the issue of acquiring CSI of users, outage probability derived for the proposed NOMA-HHN considers different types of partial CSI models. The types of partial CSI that are analyzed and compared are namely, UDI, proposed FS with DA, and with no feedback. Performance using different types of partial CSI is also compared with the conventional case of perfect CSI. Moreover, total outage probability is calculated at different tiers, which includes the tier selection probability and the RAT selection probability.
- To address the issue of initial access delay in beam training at the standalone mmWave-SBS, this work proposes FS with DA. The considered DA reduces the initial access delay in beam training, as highlighted in [13]. The proposed FS with DA uses one-bit feedback from users. However, unlike using feedback only for user ordering, as in [28], [25], feedback obtained from the users under the proposed FS serves a dual purpose: first, for user ordering, and second, for RAT selection. A comprehensive model for user ordering and RAT selection using the

proposed FS is presented in Section III. For the selected network parameters, the high SNR approximation on the analytical expression is carried out for the proposed FS, and some interesting observations are drawn. The numerical results obtained in Section VI confirms the approximations of analytical findings at high SNR.

- Another vital metric, i.e., the ergodic rate is also computed for the proposed NOMA-HHN under the assumptions of partial CSI. For a detailed insight, the outcome of the assumed partial CSI scenarios is compared with the traditional notion of perfect CSI at the BS. Moreover, energy efficiency (EE) of the proposed NOMA-HHN is studied, and some useful insights are obtained. Numerical results illustrate significant gains achieved by using the proposed NOMA-HHN over the currently deployed OMA scheme.
- The correctness of the analytical results is verified through Monte-Carlo simulations. Moreover, to corroborate the benefits of using multi-RAT SBS tier in the proposed NOMA-HHN, this work compares performance achieved by the proposed NOMA-HHN, with the traditional HetNet which deploy single RAT SBS operating at sub-6 GHz communication. The comparison between the two HetNets functioning using different technologies reveals noteworthy insights.

Rest of the paper is organized as follows. The system model is introduced in Section II. Section III discusses the proposed feedback scheme and Section IV studies the signal to interference and noise ratio (SINR) expressions. Section V derives the expressions for rate outage probability of the proposed NOMA-HHN under perfect and partial CSI. Numerical results are presented in Section VI and validated using Monte-Carlo simulations. Finally, the work concludes in Section VII.

II. System Model

A three-tier multi-RAT NOMA-HHN is considered with MBS tier, sub-6 GHz-SBS tier, and mmWave-SBS tier. The MBS tier is symbolized by c, the sub-6 GHz-SBS tier is denoted by s, and the mmWave-SBS is represented by m. The MBS tier is assumed to operate only using sub-6 GHz communication (hence, referred to as MBS tier only). The BSs, i.e., MBS tier, sub-6 GHz-SBS tier, and mmWave-SBS tier follow homogeneous Poisson point processes (PPP) distribution, denoted by Ω_c, Ω_s, and Ω_m, respectively, with corresponding intensities expressed by λ_c, λ_s, and λ_m respectively. The sub-6 GHz BSs, i.e., the MBS and the sub-6 GHz-SBS transmit using single antenna while the mmWave BSs, i.e., the mmWave-SBS are equipped with M antennas. NOMA is employed in sub-6 GHz-SBS tier and mmWave-SBS tier. The transmit power is indicated by P_c, P_s, and P_m, respectively for the MBS tier, sub-6 GHz-SBS tier and mmWave-SBS tier. Similarly, the transmission range of the BSs are represented by $\mathcal{Y}_c$, $\mathcal{Y}_s$, and $\mathcal{Y}_m$, for MBS tier, sub-6 GHz-SBS tier, and mmWave-SBS tier, respectively. The target data rate is denoted by R. The nearest neighbor (NN) connection policy is considered within each tier [30], hence, the probability density function (PDF) of the distance to the nearest BS for sub-6 GHz tiers is expressed as [31]

$$f^N_{r^t_n}(r) = 2\pi\lambda_t r e^{-\pi\lambda_t (r)^2}, \tag{1}$$

where r^t_n denotes the distance from the n^{th} user to the nearest BS of the t^{th} tier, such that $t \in \{c, s\}$ comprises of sub-6 GHz tiers. For mmWave-SBS tier, the PDF for distance to the nearest BS is discussed in Section II-B. Furthermore, it is assumed that the multi-RAT SBSs, i.e., the sub-6 GHz-SBS tier and the mmWave-SBS tier are capable of exchanging information amongst themselves [13].

***Notations*:** Throughout the paper, c, s, and m represent parameters for the MBS tier, the sub-6 GHz-SBS tier, and the mmWave-SBS tier, respectively. The superscript t indicates the set of sub-6 GHz tier, i.e., $t \in \{c, s\}$ while the superscript m denotes the parameters for the mmWave-SBS tier. When OMA is considered, the channel gains are denoted as $|\tilde{h}_c|^2$ and $|\tilde{h}_s|^2$ for the MBS tier and sub-6 GHz tier, respectively, and $|\tilde{\mathbf{h}}^*_m|^2$ is the channel gain on the beam (discussed in Section II-C) for the mmWave-SBS tier. To represent the channel gain of n^{th} user for the t^{th} tier using NOMA, this work uses $\hat{h}^t_n$ to denote Rayleigh distribution, $|\tilde{h}^t_n|^2$ to express the unordered channel gain, and $|h^t_n|^2$ to indicate the ordered channel gain. For mmWave communication, $|\tilde{\mathbf{h}}^m_n|^2$ is the channel gain of n^{th} user to nearest mmWave-SBS, whereas, $\hat{h}_m$ and $\hat{h}^m_n$ stand for Rayleigh fading while considering OMA and NOMA respectively. Moreover, while using NOMA, the unordered and ordered channel gain on the beam is represented by $|\tilde{\mathbf{h}}^*_n|^2$ and $|\mathbf{h}^*_n|^2$, respectively. Furthermore, the superscript p, d, and b represent the analysis based on the assumption of perfect CSI, UDI, and proposed FS, respectively. The operator $[\cdot]^T$ stands for the transpose, $[\cdot]^H$ represents the Hermitian transpose, $|\cdot|$ indicates the absolute value, and $\mathbb{E}[\cdot]$ denotes statistical expectation. The operator $\max\{a, b\}$ and $\min\{a, b\}$ returns the maximum and minimum of a and b, respectively.

A. sub-6 GHz Channel Model

For sub-6 GHz communication, bounded path loss model is considered [30]. The bounded path loss model for the sub-6 GHz communication is expressed as $|\tilde{h}^t_n|^2 = \frac{|\hat{h}^t_n|^2}{1+(r^t_n)^{\nu_t}}$, where $\hat{h}^t_n$ denotes small scale fading assumed to be Rayleigh distributed, r^t_n denotes the distance between the BS of the t^{th} tier and the n^{th} user, ν_t denotes the path loss exponent for the t^{th} tier.

B. mmWave Channel and Blockage Model

The channel model for the mmWave communication may be written as [4], [25]

$$\tilde{\mathbf{h}}^m_n = \sqrt{M}\frac{\hat{h}^m_n \mathbf{a}(\theta_n)}{\sqrt{1+(r^m_n)^{\nu_m}}}, \tag{2}$$

where $\nu_m = \nu^{LOS}_m$ denotes the path loss exponent for LOS path of mmWave-SBS, $\mathbf{a}(\bar{\theta}) = \frac{1}{\sqrt{M}}\left[1 \quad e^{-j\pi\bar{\theta}} \quad \cdots \quad e^{-j\pi(M-1)\bar{\theta}}\right]^T$, θ^l_n is the normalized direction of the LOS path, r^m_n is distance between the n^{th} user to the nearest mmWave-SBS, as per the NN connection

policy [4]. In (2), only line-of-sight (LOS) link is considered as argued in [25] and [32].

For blockages in the mmWave communication, this work considers probability of link to be an LOS path as $\mathcal{P}(r) = e^{-\phi r}$, where r is the link distance and ϕ depends on the density, shape, etc., of the buildings [4], [25]. The conditional PDF of distance to the nearest LOS mmWave-SBS is expressed as [4]

$$f^N_{r^m_n}(r) = \frac{2\pi\lambda_m r\mathcal{P}(r)e^{-2\pi\lambda_m \int_0^r x\mathcal{P}(x)dx}}{B_L}, \quad (3)$$

where $r > 0$ and $B_L = 1 - e^{-2\pi\lambda_m \int_0^\infty x\mathcal{P}(x)dx}$, is the probability that the user has at least one LOS mmWave-SBS.

C. Random Beamforming

As highlighted in [25], [26], the use of random beamforming reduces the system overhead hence becomes desirable for the application in mmWave communication with NOMA. The considered random beamforming can be represented as $\mathbf{p} = \mathbf{a}(\theta)$, with θ as the normalized direction uniformly distributed between -1 and 1. The beam is assumed to form a sector with central angle 2Δ. The channel gain of user on the beam can effectively be written as

$$|\tilde{\mathbf{h}}^*_n|^2 = |\tilde{h}^m_n|^2 F_M\left(\pi[\theta - \theta_n]\right), \quad (4)$$

where $|\tilde{h}^m_n|^2 = \frac{|\hat{h}^m_n|^2}{1+(r^m_n)^{\nu_m}}$, and $F_M(x)$ denotes the Fejér kernel [25], [26], [33].

D. Tier Selection Probability

The averaged biased power received (BPR) is used to determine the tier selected by the user. The BPR from the sub-6 GHz-SBS and MBS tier [30], [34] is compared and the user selects the tier with higher BPR. The probability that the sub-6 GHz-SBS tier is selected can be expressed as $\mathcal{P}_{ts} = \mathbb{E}_{r^s_n}\left[\mathcal{P}\left(B_c P_c (r^c_n)^{-\nu_c} < B_s P_s (r^s_n)^{-\nu_s}\right)\right]$. Following simple mathematics [30], the tier selection probability can be calculated as

$$\mathcal{P}_{ts} = 2\pi\lambda_s \times \int_0^{\mathcal{Y}_s} \left(e^{-2\pi\lambda_c (r^s_n)^{\frac{2\nu_s}{\nu_c}} C_1^2} - e^{-\pi\lambda_c \mathcal{Y}_c^2}\right) \times r e^{-\pi\lambda_s r^2} dr^s_n, \quad (5)$$

where $C_1 = \left(\frac{B_c P_c}{B_s P_s}\right)^{\frac{1}{\nu_c}}$.

III. Proposed Feedback Scheme using Dual Association

The conventional use of BPR applies to offloading between the tier, i.e., selection between the tiers [30], [34]. However, the proposed FS utilizes BPR for tier selection and RAT selection. The initial access delay, caused due to beamtraining using thin beams [13] at the mmWave BSs, is reduced by considering the proposed FS with DA. The DA is carried out in two steps. The first step considers the BPR from the nearest MBS and the BPR from the nearest sub-6 GHz-SBS, compares the two values, and selects the tier with higher value (detailed in Section II-D). This is followed for the tier selection and the users are offloaded from the MBS tier to the sub-6 GHz tier. It must be noted that in the first step, it is assumed that the location of users is acquired by the sub-6 GHz-SBS tier using suitable localization/signal processing techniques [35]. Given suitable technique, the sub-6 GHz-SBS and the mmWave-SBSs are co-located [14], and the information regarding users' location can be shared by the mmWave-SBS, it may be utilized to calculate the coarse-grained angle information for beamtraining. This can considerably reduce the initial access delay at the mmWave front end [12]. Furthermore, the second step in the DA deals with RAT selection. In this context, the BPR of the nearest sub-6 GHz-SBS and the BPR of the nearest mmWave-SBS is compared. The RAT with higher BPR is selected by the user (detailed in Section III-A), thereby completing the second step of the proposed FS with DA.

It is interesting to note that the proposed FS with DA differs from the conventional scheme where the BPR of all the tiers and RATs are compared in a single step [36]. The advantage of using the two-step association is to reduce the access delay at the mmWave-SBS tier [13]. Since the users' location information gathered in the first step is shared by the mmWave-SBS which aids in speedy calculations at the mmWave front end for beamtraining.

A. RAT selection using Proposed FS

The RAT selection is performed by comparing the BPR from the nearest sub-6 GHz-SBS and from the nearest mmWave-SBS. The user is connected by the SBS with higher BPR. Accordingly, bit "0" is transmitted by the user if the BPR from the nearest sub-6 GHz-SBS is higher otherwise bit "1" is transmitted if the BPR from the nearest mmWave-SBS is higher. The feedback received from the user decides which RAT it will connect with. Mathematically, the RAT selection probability is expressed as

$$\begin{aligned}\mathcal{P}_m &= \mathbb{E}_{r^m_n}\left[\mathcal{P}\left(B_s P_s (r^s_n)^{-\nu_s} < B_m P_m (r^m_n)^{-\nu_m}\right)\right] \\ &= \mathbb{E}_{r^m_n}\left[\mathcal{P}\left(r^s_n > \left(\frac{B_s P_s}{B_m P_m}\right)^{\frac{1}{\nu_s}} (r^m_n)^{\frac{\nu_m}{\nu_s}}\right)\right] \\ &\overset{(a)}{=} \mathbb{E}_{r^m_n}\left[\left(e^{-2\pi\lambda_m (r^m_n)^{\frac{2\nu_m}{\nu_s}} C_2^2} - e^{-\pi\lambda_s \mathcal{Y}_s^2}\right)\right], \quad (6)\end{aligned}$$

where $C_2 = (B_s P_s / B_m P_m)^{\frac{1}{\nu_s}}$ and (a) is derived using PDF of r^s_n. Taking expectation over r^m_n, PDF for which is given in (3), the probability of user transmitting bit "1", i.e., connecting to mmWave-SBS is expressed as

$$\mathcal{P}_m = \int_0^{\mathcal{Y}_m} \left(e^{-2\pi\lambda_m (r)^{\frac{2\nu_m}{\nu_s}} C_2^2} - e^{-\pi\lambda_s \mathcal{Y}_s^2}\right) f^N_{r^m_n}(r) dr. \quad (7)$$

Similarly, probability of user connecting to sub-6 GHz-SBS is calculated as $\mathcal{P}_s = 1 - \mathcal{P}_m$.

B. User Scheduling using Proposed FS

Under the proposed FS, user scheduling is performed using feedback from the users. The sub-6 GHz-SBS and mmWave-SBS broadcast a pre-defined threshold, denoted by ζ_s and ζ_m, respectively. Assuming users perfectly know their CSI, each user compares its channel gain with the broadcasted threshold. On comparing, the user sends bit "0", if the channel gain at the user is smaller than the threshold. Whereas, bit "1" is fed if the channel gain is higher than the broadcasted threshold.

Accordingly, the users are classified as Group-0 (Gr-0) user for the former case and as Group-1 (Gr-1) user for the later. For NOMA, users are paired by selecting one user randomly from Gr-0 and one randomly from Gr-1.

It must be noted that the use of one-bit feedback is advantageous only when the selected pre-defined threshold is carefully chosen. A poor selection of threshold may prove disadvantageous. For instance, if the selected threshold is very small, it may render a user with poor channel condition to be a strong user. Likewise, a large threshold may decide a strong user to be a weak user. Thus, it is important to select an appropriate threshold for user scheduling. From the existing literature in [25], [28], threshold should decrease with the SNR.

IV. SINR ANALYSIS

This section calculates SINR at typical user for all the considered tiers. Further, SINR using both OMA and NOMA is calculated for a comparative study.

A. MBS and sub-6 GHz-SBS using OMA

Let the signal intended for a user of MBS tier and sub-6 GHz-SBS tier be denoted by x_t, such that $t \in \{c, s\}$. The signal transmitted by the BS and received at user can be written as $X_t^{tx} = \sqrt{P_t}x_t$ and $X_t^{rx} = X_t^{tx}\tilde{h}_t + w_t$, respectively, where w_t denotes noise. Hence, the SINR at a typical user of t^{th} tier may be expressed as

$$\gamma_t = \frac{P_t|\tilde{h}_t|^2\mathbb{E}\left[x_t^2\right]}{\sum_t P_t\mathcal{I}_t + \sigma_t^2}, \tag{8}$$

where $P_t\mathcal{I}_t$ denotes interference from the t^{th} tier. Assuming Slivnyak's theorem [37] and the tagged MBS to be c_0 when the user connects to the MBS tier, the co-tier interference from MBS tier to the user can be written as $\mathcal{I}_c = \sum_{i\in\Omega_c/\{c_0\}}|\tilde{h}_i^c|^2$, where $|\tilde{h}_i^c|^2$ denotes the total channel gain from i^{th} MBS to the user, and the cross-tier interference from the sub-6 GHz tier is given as $\mathcal{I}_s = \sum_{j\in\Omega_s}|\tilde{h}_j^s|^2$, where $|\tilde{h}_j^s|^2$ represents the total channel gain from j^{th} sub-6 GHz-SBS to user. Similarly, assuming the tagged sub-6 GHz-SBS to be s_0 when the user connects to the sub-6 GHz tier, the co-tier interference from sub-6 GHz-SBS tier to the user is expressed as $\mathcal{I}_s = \sum_{i\in\Omega_s/\{s_0\}}|\tilde{h}_i^s|^2$, where $|\tilde{h}_i^s|^2$ denotes the total channel gain from i^{th} sub-6 GHz-SBS to the user, and the cross-tier interference from the MBS tier is given as $\mathcal{I}_c = \sum_{j\in\Omega_c}|\tilde{h}_j^c|^2$, where $|\tilde{h}_j^c|^2$ represents the total channel gain from j^{th} MBS to the user. σ_t^2 indicates noise variance. Normalizing the equation by dividing both, numerator and denominator by σ_t^2, we get the SINR in terms of transmit signal to noise ratio (SNR) of the t^{th} tier (ρ_t) as

$$\gamma_t = \frac{P_t\rho_t^o|\tilde{h}_t|^2}{\sum_t \rho_t^I\mathcal{I}_t + 1}, \tag{9}$$

where $\rho_t^o = \mathbb{E}\left[x_t^2\right]/\sigma_t^2$. The $\rho_t^I = P_t/\sigma_t^2$, such that $t \in \{c, s\}$ expresses the transmit SNR from interfering MBS tier and sub-6 GHz-SBS, respectively.

B. sub-6 GHz-SBS Tier with NOMA

Assuming N users with their channel gains ordered as $|h_1^s|^2 \leq \cdots \leq |h_N^s|^2$. Given x_n as the signal for the n^{th} user and $\mathbb{E}[x_n^2]$ to be equal $\forall i \in (1, 2, \cdots, N)$. The signal transmitted by the sub-6 GHz-SBS is given by $X_{s,n}^{tx} = \sum_{i=1}^{N} x_n\sqrt{a_nP_s}$ and the signal received by user n is given by $X_{s,n}^{rx} = h_n^sX_{s,n}^{tx} + w_s$. To decode message of user j ($j < n$), the SINR at user n is given as [38]

$$\gamma_{n\to j}^s = \frac{\rho_sP_sa_j|h_n^s|^2}{\rho_sP_s|h_n^s|^2\sum_{l=j+1}^{N}a_l + \sum_t\rho_t^I\mathcal{I}_t + 1}, \tag{10}$$

where $\rho_s = \mathbb{E}[x_n^2]/\sigma_s^2$ is the transmit SNR at sub-6 GHz-SBS and a_n is the power allocated to user n. To decode the self message, the SINR at user n is given by

$$\gamma_n^s = \frac{\rho_sP_sa_n|h_n^s|^2}{\rho_sP_s|h_n^s|^2\sum_{l=k+1}^{N}a_l + \sum_t\rho_t^I\mathcal{I}_t + 1}. \tag{11}$$

C. mmWave-SBS Tier with OMA

The mmWave-SBS transmits the signals on a beam as $X_{m,tx} = \mathbf{p}\left(P_mx_m\right)$. The received signal can be described as $X_{m,rx} = \tilde{\mathbf{h}}_m^*X_{m,tx} + w_m$, where w_m denotes AWGN. Thus, the SINR at user from mmWave-SBS using OMA is formulated as $\gamma_m = P_m|\tilde{\mathbf{h}}_m^*|^2\rho_m^o$, where $\rho_m^o = \frac{\mathbb{E}[x_m^2]}{\sigma_m^2}$ and σ_m^2 denotes the noise variance.

D. mmWave-SBS Tier with NOMA

Assuming the mmWave-SBS superimposes the signals of N users on the beam as $X_{tx}^m = \mathbf{p}\left(\sum_{n=1}^{n=N}a_nx_n\right)$. The received signal at the n^{th} user is given as $X_{rx}^m = \mathbf{h}_n^*X_{tx}^m + w_m$. To decode message of user j ($j < n$), the SINR at user n is calculated as

$$\gamma_{n\to j}^m = \frac{\rho_ma_j|\mathbf{h}_n^*|^2}{\rho_m|\mathbf{h}_n^*|^2\sum_{l=j+1}^{N}a_l + 1}, \tag{12}$$

where $\rho_m = \frac{\mathbb{E}[x_n^2]}{\sigma_m^2}$. To decode its own message, the SINR at user n is given by

$$\gamma_n^m = \frac{\rho_ma_n|\mathbf{h}_n^*|^2}{\rho_m|\mathbf{h}_n^*|^2\sum_{l=k+1}^{N}a_l + 1}. \tag{13}$$

Since, mmWave communication is directional and employs beamforming, it is valid to assume that the mmWave communication is noise limited as also discussed in [3]. Therefore, interference is not considered in this work.

V. RATE OUTAGE PROBABILITY ANALYSIS

This section evaluates the expressions for the rate outage probability for the MBS tier, the sub-6 GHz-SBS tier, and the mmWave-SBS tier. Rate outage probability is defined as the probability that the rate at a typical user is greater than a rate threshold [34]. The rate outage probability is derived using OMA and NOMA. Furthermore, the calculations are performed under perfect CSI and partial CSI scenarios. The partial CSI scenarios considered are namely, UDI and the proposed FS.

A. MBS Tier and sub-6 GHz-SBS Tier with OMA

A user connects to the nearest BS of the t^{th} tier such that $t \in \{c, s\}$. The cumulative distribution function (CDF) of the unordered channel gain can be expressed as [39]

$$F_{|\tilde{h}_t|^2}(y) = 2\pi\lambda_t \int_0^{\mathcal{Y}_t} \left(1 - e^{-(1+r_t^{\nu_t})y}\right) e^{-2\pi\lambda_t r_t^2} r_t dr_t. \tag{14}$$

Using Gaussian Chebyshev (GC) quadrature [40], (14) may be approximated as

$$F_{|\tilde{h}_t|^2}(y) \approx \pi\lambda_t \mathcal{Y}_t^2 \sum_{z=0}^{Z} b_z^t e^{-c_z^t y}, \tag{15}$$

where Z is GC quadrature parameter, $c_z^t = 1 + \left(\frac{\mathcal{Y}_t}{2}\theta_z + \frac{\mathcal{Y}_t}{2}\right)^{\nu_t}$, $c_0^t = 0$, $w_Z = \frac{\pi}{Z}$, $\theta_z = \cos\left(\frac{2z-1}{2Z}\pi\right)$, $b_z^t = -w_Z\sqrt{1-\theta_z^2}(\frac{1}{2}(\theta_z+1))e^{-\pi\lambda_S\left(\frac{1}{2}(\theta_z+1)\mathcal{Y}_t\right)^2}$, $b_0^t = -\sum_{z=1}^{Z} b_z^t$, [39]. The outage probability of user of the t^{th} tier is given as

$$\mathcal{O}_t = \pi\lambda_S \mathcal{Y}_t^2 \sum_{z=0}^{Z} b_z^t e^{-c_z^t \frac{\phi^o}{\rho_t P_t}} \prod_t \mathcal{L}_{\mathcal{I}_t}(s_t^O \rho_t),$$

where $s_t^o = \frac{c_z^t \phi^o}{\rho_t}$, $\phi^o = 2^{2R} - 1$, and $\mathcal{L}_{\mathcal{I}_s}(s)$ is the Laplace transform (LT) of interference from the t^{th} tier and is calculated as [41], $\mathcal{L}_{\mathcal{I}_t}(s) = e^{\pi\lambda_t\left(s^{\delta_t}\Gamma(1-\delta_t,s) - s^{\delta_t}\Gamma(1-\delta_t)\right)}$, where $\delta_t = 2/\nu_t$, $\Gamma(a,x) = \int_x^\infty t^{a-1}e^{-t}dt$ and $\Gamma(a) = \int_0^\infty x^{a-1}e^{-x}dx$.

B. sub-6 GHz-SBS Tier with NOMA

This section derives expression for the outage probability for the sub-6 GHz-SBS tier with NOMA using perfect CSI, UDI, and the proposed FS.

1) Using perfect CSI: CDF of unordered channel gain of sub-6 GHz-SBS tier is given as

$$F_{|\tilde{h}_n^s|^2}(y) = \int_0^{\mathcal{Y}_s} \left(1 - e^{-(1+(r)^{\nu_s})y}\right) f_{r_n^s}^N(r) dr. \tag{16}$$

Using GC quadrature [40], (16) can be approximated as

$$F_{|\tilde{h}_n^s|^2}(y) \approx \pi\lambda_s \mathcal{Y}_s^2 \sum_{z=0}^{Z} b_z^s e^{-c_z^s y}, \tag{17}$$

The ordered channel gain of sub-6 GHz-SBS tier is related with the unordered channel gain of sub-6 GHz-SBS tier $F_{|\tilde{h}_n^s|^2}^p(y)$ as given by [38]

$$F_{|h_n^s|^2}^p(y) = \psi_n \sum_{k=0}^{N-n} \binom{N-n}{k} \frac{(-1)^k}{n+k} \left(F_{|\tilde{h}_n^s|^2}(y)\right)^{k+n}, \tag{18}$$

where $\psi_n = \frac{N!}{(n-1)!(N-n)!}$ and the binomial coefficient is given as $\binom{N-n}{k} = \frac{(N-n)!k!}{(N-n-k)!}$. Substituting (17) in (18) and applying multinomial theorem, we get the CDF of ordered channel gain as

$$F_{|h_n^s|^2}^p(y) = \psi_n \sum_{k=0}^{N-n} \binom{N-n}{k} \frac{(-1)^r}{n+k} \sum_{T_n^k} \binom{n+k}{q_0 \cdots q_Z} \left(\prod_{z=0}^{Z} (b_z^s)^{q_z}\right) e^{-\sum_{z=0}^{Z} q_z c_z^s y}, \tag{19}$$

where, $T_n^k = \left(q_0! \cdots q_Z! \mid \sum_{i=0}^{Z} q_i = n+k\right)$, $\binom{n+k}{q_0 \cdots q_Z} = \frac{N!}{q_0! \cdots q_Z!}$. Assuming the channel gains of N users to be ordered as $|h_1^s|^2 \leq \cdots \leq |h_N^s|^2$, since the outage probability is decided on successful SIC followed by successful decoding of self message, the outage probability at user n is derived as $\mathcal{O}_n^{s,p} = 1 - \mathcal{P}\left(\log_2(1+\gamma_{n\to j}^s) > R, \log_2(1+\gamma_n^s) > R\right) = 1 - \mathcal{P}\left(\gamma_{n\to j}^s > \phi, \gamma_n^s > \phi\right)$, where $\phi = 2^R - 1$. Thus, the outage probability of user n can be written as

$$\mathcal{O}_n^{s,p} = \mathcal{P}\left(|h_n^s|^2 < \epsilon_{max}^s(1 + \sum_t \rho_t^I \mathcal{I}_t)\right), \tag{20}$$

where $\epsilon_{max}^s = \max\left(\epsilon_1^s, \epsilon_2^s, \ldots, \epsilon_n^s\right)$ such that ϵ_n^s is calculated as $\epsilon_n^s = \phi/(\rho_s \times (a_n - \phi\sum_{i=n+1}^{N} a_i))$. This gives the outage probability as $\mathcal{O}_n^{s,p} = F_{|h_n^s|^2}^p(y_n^{s,p})$, where $y_n^{s,p} = \epsilon_{max}^s(1 + \sum_t \rho_t^I \mathcal{I}_t)$. Hence, the outage probability of user n can be calculated as

$$\mathcal{O}_n^{s,p} = \psi_n \sum_{k=0}^{N-n} \binom{N-n}{k} \frac{(-1)^k}{n+k} \sum_{T_n^k} \binom{n+k}{q_0 \cdots q_Z} \left(\prod_{n=0}^{Z} b_z^{s\,q_z}\right) e^{-\sum_{z=0}^{Z} q_z c_z^s \frac{\epsilon_{max}}{\rho_s}} \prod_t \mathcal{L}_{\mathcal{I}_t}(s_s \rho_t^I). \tag{21}$$

2) Using UDI:

Proposition 1: The outage probability using UDI can be expressed as $\mathcal{O}_n^{s,d} = F_{|h_n^s|^2}^d(y_n^{s,d})$, where $y_n^{s,d} = \epsilon_{max}^s(1 + \sum_t \rho_t^I \mathcal{I}_t)$, the CDF of the channel gain ordered using UDI is evaluated as

$$F_{|h_n^s|^2}^d(z) = \mathcal{P}\left\{\frac{|h_n^s|^2}{(r_n^s)^{\nu_s}} \leq z\right\} = \int_0^{\mathcal{Y}_s} (1 - e^{-zr^{\nu_s}}) f_{r_n^s}^d(r) dr, \tag{22}$$

where $f_{r_n^s}^d(r)$ is the PDF of the Euclidean distance r_n^s of the n^{th} nearest user from the sub-6 GHz-SBS and is expressed as follows

$$f_{r_n^s}^d(r) = 2n\binom{N}{n} \sum_{j=0}^{N-n} \binom{N-n}{j} (-1)^j \frac{r^{2(n+j)-1}}{\mathcal{Y}_s{}^{2(n+j)}}. \tag{23}$$

Proof: Please see Appendix A.

3) Using proposed FS:

Proposition 2:

The outage probability of a user in Gr-0 can be expressed as

$$\mathcal{O}_0^{s,f} = \sum_{z=0}^{Z} b_z^s e^{-s_0^s} \mathcal{L}_{\mathcal{I}_s}(s_0^s \rho_s^I) \mathcal{L}_{\mathcal{I}_c}(s_0^s \rho_c^I) / \sum_{z=0}^{Z} b_z^s e^{-c_z^s \zeta_s}, \tag{24}$$

where $s_0^s = c_z^s \epsilon_1^s$. For user in Gr-1, the outage probability can be calculated as

$$\mathcal{O}_1^{s,f} = \sum_{z=0}^{Z} b_z e^{-s_1^s} \mathcal{L}_{\mathcal{I}_s}(s_1^s \rho_s^I) \mathcal{L}_{\mathcal{I}_c}(s_1^s \rho_c^I) - \mathcal{X}/(1-\mathcal{X}), \tag{25}$$

where $\mathcal{X} = \sum_{z=0}^{Z} b_z e^{-c_z^s \zeta_s}$ and $s_1^s = c_z^s \epsilon_{max}^s$, and $\epsilon_{max}^s = \max(\epsilon_1^s, \epsilon_2^s)$.

Proof: Please see Appendix B.

C. mmWave-SBS Tier with OMA

The effective channel gain of a user on the randomly generated beam is expressed by $|\tilde{\mathbf{h}}_m^*|^2 = |\tilde{h}_m|^2 F_M^o(\pi[\theta - \theta_m])$,

where $|\tilde{h}_m|^2 = \frac{|\hat{h}_m|^2}{1+(r_n^m)^{\nu_m}}$ and $F_M^o(\pi[\theta-\theta_m]) = F_M(\pi[\theta-\theta_m])$. The CDF of channel gain for mmWave-SBS tier may be obtained as

$$F_{|\tilde{\mathbf{h}}_\mathbf{m}^*|^2}(y) \approx \int_{\theta-\Delta}^{\theta+\Delta}\int_0^{\mathcal{Y}_m}\left(1-e^{-\frac{y(1+(r)^{\nu_m})}{F_M^o(\pi[\theta-\theta_m])}}\right)\frac{f_{r_m}^N(r)}{2\Delta}drd\theta_t. \tag{26}$$

Using the SINR at user from mmWave-SBS using OMA, the outage probability is expressed as $\mathcal{O}_m = \mathcal{P}(\gamma_m < \eta)$. Hence, the outage probability is calculated as $\mathcal{O}_m = F_{|\tilde{\mathbf{h}}_\mathbf{m}^*|^2}(y_m^o)$, where $y_m^o = \phi^o/\rho_m$.

D. mmWave-SBS Tier with NOMA

This section derives the expression for the outage probability for the mmWave-SBS tier with NOMA using perfect CSI, UDI, and the proposed FS.

1) Using perfect CSI: The ordered channel gain of mmWave-SBS tier is related with the unordered channel gain of mmWave-SBS tier $F_{|\tilde{\mathbf{h}}_\mathbf{n}^*|^2}(y)$ given by [38]

$$F_{|\mathbf{h}_\mathbf{n}^*|^2}^p(y) = \psi_n\sum_{k=0}^{N-n}\binom{N-n}{k}\frac{(-1)^k}{n+k}\left(F_{|\tilde{\mathbf{h}}_\mathbf{n}^*|^2}(y)\right)^{k+n}, \tag{27}$$

where the CDF of unordered channel gain of mmWave-SBS tier is expressed as

$$F_{|\tilde{\mathbf{h}}_\mathbf{n}^*|^2}(y) \approx \int_{\theta-\Delta}^{\theta+\Delta}\int_0^{\mathcal{Y}_m}\left(1-e^{-\frac{y(1+(r)^{\nu_m})}{F_M}}\right)\frac{f_{r_n^m}^N(r)}{2\Delta}drd\theta_n, \tag{28}$$

such that F_M represents the the Fejér kernel when Δ approaches zero as is approximated as

$$F_M(\pi[\theta-\theta_n]) \approx M\left(1-\frac{\pi^2M^2(\theta-\theta_n)^2}{12}\right) = F_M. \tag{29}$$

For n^{th} user, the outage probability can be calculated using the SINR in (12) and (13) as

$$\mathcal{O}_n^{m,p} = 1-\mathcal{P}\left(\gamma_{n\to j}^m > \phi, \gamma_n^m > \phi\right) \tag{30}$$

Hence, the outage probability is calculated as $\mathcal{O}_n^{m,p} = F_{|\mathbf{h}_\mathbf{n}^*|^2}^p(y_n^{m,p})$, where $y_n^{m,p} = \epsilon_{max}^m$, $\epsilon_{max}^m = \max\{\epsilon_1^m, \epsilon_1^m, \cdots, \epsilon_n^m\}$, and $\epsilon_n^m = \phi/(\rho_m \times (a_n - \phi\sum_{i=n+1}^N a_i))$.

2) Using UDI:

Proposition 3: Assuming that the distance of the users from the tagged mmWave-SBS is available, the outage probability of the n^{th} user can be expressed as

$$\mathcal{O}_n^{m,d} = F_{|\mathbf{h}_n^*|^2}^d(y_n^{m,d}), \tag{31}$$

where $y_n^{m,d} = \epsilon_{max}^m$ and the CDF of the ordered channel gain with UDI is expressed by

$$F_{|\mathbf{h}_n^*|^2}^d(z) = \int_0^{\mathcal{Y}_m}(1-e^{\frac{-zr^{\nu_m}}{F_M}})f_{r_n^m}^d(r)dr, \tag{32}$$

such that the PDF of distance of the n^{th} nearest user from the mmWave-SBS is given as

$$f_{r_n^m}^d(r) = 2n\tbinom{N}{n}\sum_{j=0}^{N-n}\tbinom{N-n}{j}(-1)^j\frac{r^{2(n+j)-1}}{{\mathcal{Y}_m}^{2(n+j)}}. \tag{33}$$

Proof: Please see Appendix C.

3) Using proposed FS:

Proposition 4: The outage probability of user in Gr-0 can be calculated as

$$\mathcal{O}_0^{m,f} = F_0^{m,f}(y_0^{m,f}), \tag{34}$$

where $y_0^{m,f} = \epsilon_1^m$, and the CDF of channel gain for Gr-0 user is given as

$$F_0^{m,f}(y) = \frac{F_{|\mathbf{h}_\mathbf{n}^*|^2}(\min\{y,\zeta_m\})}{F_{|\mathbf{h}_\mathbf{n}^*|^2}(\zeta_m)}, \tag{35}$$

such that $F_{|\mathbf{h}_\mathbf{n}^*|^2}(y)$ is given in (28). For user in Gr-1, the outage probability may be written as

$$\mathcal{O}_1^{m,f} = F_1^{m,f}(y_1^{m,f}), \tag{36}$$

where $y_1^{m,f} = \epsilon_{max}^m$, and $\epsilon_{\max}^m = \max\{\epsilon_1^m, \epsilon_2^m\}$. The CDF of channel gain for Gr-1 user is expressed as follows for $y > \zeta_m$, since, for $y < \zeta_m$ $F_1^{m,f}(y) = 0$.

$$F_1^{m,f}(y) = \frac{\mathcal{P}\left(\zeta_m < |\mathbf{h}_\mathbf{n}^*|^2 < y\right)}{\mathcal{P}\left(|\mathbf{h}_\mathbf{n}^*|^2 > \zeta_m\right)} = \frac{F_{|\mathbf{h}_\mathbf{n}^*|^2}(y) - F_{|\mathbf{h}_\mathbf{n}^*|^2}(\zeta_m)}{1-F_{|\mathbf{h}_\mathbf{n}^*|^2}(\zeta_m)}. \tag{37}$$

Proof: Please see Appendix D.

E. High SNR Approximation and Diversity Analysis

Assuming that at high SNR y tends to zero, using the Taylor series expansion for the exponential function, and utilizing the fact that $1-e^{-x} \approx x$ when $x \to 0$, $F_{|\tilde{h}_n^s|^2}(y)$ in (16) may be approximated as

$$F_{|\tilde{h}_n^s|^2}^\infty(y) \approx \int_0^{\mathcal{Y}_s}(1+r^{\nu_s})y \times f_{r_n^s}^N(r)dr = c_s \times y, \tag{38}$$

where $c_s = \int_0^{\mathcal{Y}_s}(1+r^{\nu_s}) \times f_{r_n^s}^N(r)dr$.

1) Diversity gain analysis of Gr-0 and Gr-1 user for sub-6 GHz-SBS tier: The CDF of channel gain for Gr-0 user is approximated, at high SNR, as follows

$$F_0^{s,\infty}(y) = \frac{F_{|\tilde{h}_n^s|^2}^\infty(\min\{y,\zeta_s\})}{F_{|\tilde{h}_n^s|^2}^\infty(\zeta_s)} \approx \frac{\min\{y,\zeta_s\}}{\zeta_s}. \tag{39}$$

Correspondingly, at high SNR, the outage probability of user in Gr-0 is given as

$$\mathcal{O}_0^{s,\infty} = F_0^{s,\infty}(y_0^{s,f}) \approx \frac{\min\{y_0^{s,f},\zeta_{s,f}\}}{\zeta_u}. \tag{40}$$

Remark 1: Since, $y_0^{s,f}$ approaches zero at high SNR, this implies that $\min\{y_0^{s,f},\zeta_s\}$ also approaches zero at high SNR at the same rate [25]. Furthermore, the selected value of ζ_s decreases with ρ_s as $\zeta_s \dot{\sim} \frac{1}{\rho_s}$, [25], [28], where the operator $\dot{\sim}$ can be interpreted as "is approximately distributed as". Hence, (40) implies that the outage probability of user in Gr-0 becomes independent of ρ_s at high SNR. Therefore, we find that asymptotically there is an error floor in the outage probability of Gr-0 user, as is evident from Section VI, which verifies the high SNR approximation results in (40).

Using the high SNR approximation from (38), the CDF of channel gain for Gr-1 user may be approximated as

$$F_1^{s,\infty}(y) = \frac{F^{\infty}_{|\tilde{h}_n^s|^2}(y) - F^{\infty}_{|h_n^s|^2}(\zeta_s)}{1 - F^{\infty}_{|\tilde{h}_n^s|^2}(\zeta_s)} \approx c_s \times \max\{0, (y - \zeta_s)\}. \tag{41}$$

The outage probability for Gr-1 user is calculated as

$$\mathcal{O}_1^{s,\infty} = F_1^{s,\infty}(y_1^{s,f}) \approx c_s \times \max\{0, \left(y_1^{s,f} - \zeta_s\right)\} \dot{\sim} \frac{1}{\rho_u}. \tag{42}$$

This gives the diversity gain for Gr-1 user as 1, as can also be observed from Section VI, which verifies the analytical findings.

2) Diversity gain analysis of Gr-0 and Gr-1 user for mmWave-SBS tier: Similar to Section V-E1, the CDF in (28) may be approximated as

$$F^{\infty}_{|\mathbf{h}_n^*|^2}(y) \approx \int_{\theta-\Delta}^{\theta+\Delta} \int_{0}^{\mathcal{Y}_m} \left(\frac{y(1 + r^{\nu_m})}{F_M}\right) \frac{f^N_{r_n^m}(r)}{2\Delta} dr d\theta_n \approx c_m \times y, \tag{43}$$

where $c_m = \int_{\theta-\Delta}^{\theta+\Delta} \int_{0}^{\mathcal{Y}_m} \left(\frac{(1+r^{\nu_m})}{F_M}\right) \frac{f^N_{r_n^m}(r)}{2\Delta} dr d\theta_n$. Therefore, CDF for channel gain of user in Gr-0 may be approximated as

$$F_0^{m,\infty}(y) = \frac{F^{\infty}_{|\mathbf{h}_\mathbf{n}^*|^2}(\min\{y, \zeta_m\})}{F^{\infty}_{|\mathbf{h}_\mathbf{n}^*|^2}(\zeta_m)} \approx \frac{\min\{y, \zeta_m\}}{\zeta_m}. \tag{44}$$

At high SNR, $y_0^{m,f}$ approaches zero, thus, using (44), the outage probability at Gr-0 user is approximated as

$$\mathcal{O}_0^{m,\infty} = F_0^{m,\infty}(y_0^{m,f}) \approx \frac{\min\{y_0^{m,f}, \zeta_m\}}{\zeta_m}. \tag{45}$$

Remark 2: Since, $y_0^{m,f}$ approaches zero at high SNR, this implies that $\min\{y_0^{m,f}, \zeta_m\}$ also approaches zero at high SNR with the same rate [25]. Moreover, the selected value of ζ_m decreases with ρ_m as $\zeta_m \dot{\sim} \frac{1}{\rho_m}$, [25], [28]. Hence, (45) implies that the outage probability of user in Gr-0 becomes independent of ρ_m at high SNR. Therefore, we find that asymptotically the outage probability of Gr-0 user approaches error floor, as is evident from Section VI, which verifies the analytical findings using high SNR approximation.

Again, when SNR is high, $y_1^{m,f}$ approaches zero, using (43), the CDF of user in Gr-1 is approximated as

$$F_1^{m,\infty}(y) = \frac{F^{\infty}_{|\mathbf{h}_\mathbf{n}^*|^2}(y) - F^{\infty}_{|\mathbf{h}_\mathbf{n}^*|^2}(\zeta_m)}{1 - F_{|\mathbf{h}_\mathbf{n}^*|^2 \infty}(\zeta_m)} \approx c_m \max\{0, (y - \zeta_m)\}. \tag{46}$$

Using (46), the high SNR approximation for outage probability for Gr-1 user is expressed as

$$\mathcal{O}_1^{m,\infty} \approx c_m \max\{0, (y_1^{m,f} - \zeta_m)\} \dot{\sim} \frac{1}{\rho_m}. \tag{47}$$

This gives the diversity gain for Gr-1 user as 1.

F. Total Tier-Outage Probability

In this section, we calculate the total tier-outage probability of each tier by performing, offloading and RAT selection under perfect CSI, UDI, and the proposed FS. After offloading, the outage probability at the MBS tier is given as $(1 - \mathcal{P}_{ts})\mathcal{P}_c$.

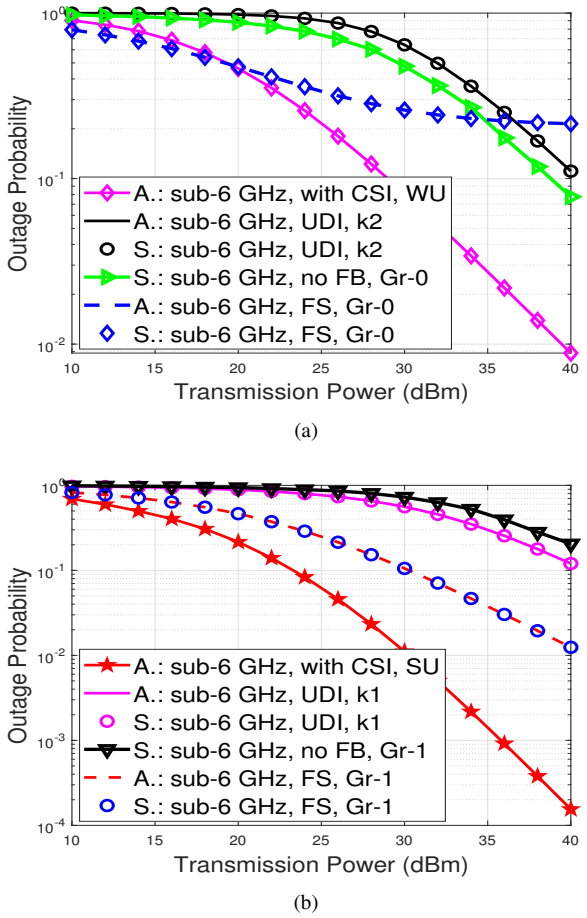

Fig. 1: Outage probability at sub-6 GHz-SBS using partial CSI (a) For Gr-0 user. (b) For Gr-1 user.

After offloading and RAT selection, the outage probabilities at sub-6 GHz-SBS tier and mmWave-SBS tier are calculated as $\mathcal{P}_{ts}\mathcal{P}_m\mathcal{O}_n^{s,p}$ and $\mathcal{P}_{ts}(1-\mathcal{P}_m)\mathcal{O}_n^{s,p}$, respectively, using perfect CSI at the BS. Similarly, with UDI, the tier outage probability at the sub-6 GHz-SBS tier and mmWave-SBS tier with offloading and RAT selection are calculated as $\mathcal{P}_{ts}\mathcal{P}_m\mathcal{O}_n^{s,d}$ and $\mathcal{P}_{ts}(1-\mathcal{P}_m)\mathcal{O}_n^{s,d}$, respectively, and using the proposed FS it is given as $\mathcal{P}_{ts}\mathcal{P}_m\mathcal{O}_n^{s,f}$ and $\mathcal{P}_{ts}(1-\mathcal{P}_m)\mathcal{O}_n^{s,f}$, respectively.

VI. Results and Discussions

This section analyzes the rate outage probability based on the analytical expressions derived in Section V. The system parameters considered to analyze the outage probabilities are $\lambda_c = 10^{-5}$, $\lambda_s = 5 \times 10^{-4}$, $\lambda_m = 5 \times 10^{-3}$, $B_c = B_s = 1$, $B_m = 3$, $\mathcal{Y}_c = 1$km, $\mathcal{Y}_s = 100$m, $R = 0.1$ bps, $\nu_c = 3.5$, $\nu_s = 3$, $\nu_m = 2$, $\mathcal{Y}_m = 10$m, $\phi = 0.01$, $\Delta = 0.01$, $M = 4$, $N = 10$, $\zeta_s = \frac{1}{\rho_s}$, $\zeta_m = \frac{1}{\rho_m}$[1]. The selected parameters are

[1]The CDF in (54) implies that the outage probability at Gr-0 user for $\zeta_s < y_0^{s,f}$ is always equal to 1, i.e., for $\zeta_s < y_0^{s,f}$ the user in Gr-0 always experiences outage. When the transmit SNR approaches infinity, then $y_0^{s,f}$ approaches zero, i.e., $y_0^{s,f} \to 0$. This means that $\min\{y_0^{s,f}, \zeta_s\}$ is always ζ_s leading outage probability to 1. To avoid such situation, at high SNR, threshold should also approach 0, i.e, $\zeta_s \to 0$, this makes the value of predefined threshold inversely proportional to transmit SNR a viable choice.

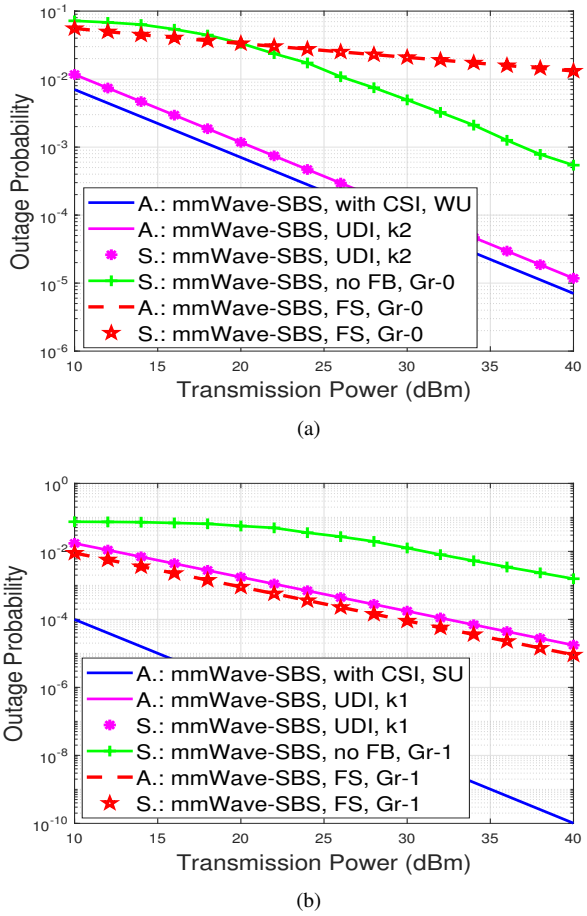

Fig. 2: Outage probability at mmWave-SBS tier using partial CSI (a) For Gr-0 user. (b) For Gr-1 user.

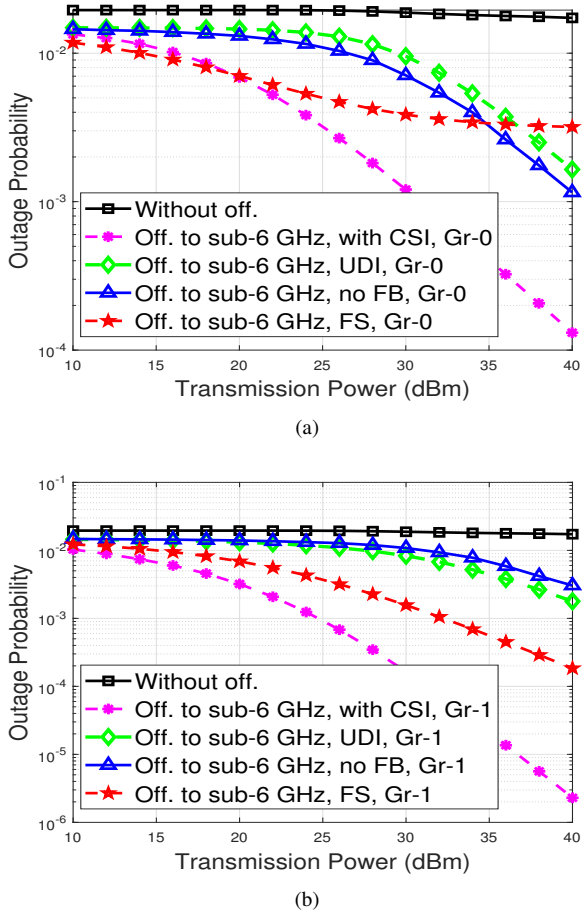

Fig. 3: Tier-outage probability at sub-6 GHz-SBS after offloading and RAT selection(a) For Gr-0 user. (b) For Gr-1 user.

similar to the ones used in [25], [28], [30], and [34]. For a comparative analysis, the following benchmarks are used: (i) using perfect CSI at BSs, (ii) with UDI, (iii) using proposed FS, and (iv) with no CSI feedback. The scenario with no CSI feedback indicates that the BS orders the users randomly due to lack of information regarding the actual CSI [21]. The no feedback case is a special case of the considered feedback with $\zeta_r = 0$ or $\zeta_r = \infty$, such that $r \in \{s, m\}$. Furthermore, the tier outage probability with and without offloading is plotted for the proposed NOMA-HHN. Comparisons are carried out at transmission power of 30dBm for the sub-6 GHz and mmWave SBSs. The analytical results are denoted by "A." while the simulation curves are represented by "S.".

Fig. 1 and Fig. 2 show the outage probability of Gr-0 and Gr-1 user at sub-6 GHz-SBS and mmWave-SBS tier using partial CSI, respectively. The partial CSI used are namely, with UDI, i.e., when information of users' distance is known at the BS, when no feedback (abbreviated as no FB in the figures) is available at the BS, and using the proposed FS. Fig. 1(a) shows the outage probability of Gr-0 user at the sub-6 GHz-SBS tier. It can be observed from Fig. 1(a) that perfect CSI forms the lower bound (ideal) on the outage probability for the user. Outage probability using proposed FS shows the best performance and achieves enhancement of 59.63% when compared to the outage probability with UDI and improvement of 45.68% is observed when compared to no feedback scenario. Ordering of users using only distance information does not guarantee same ordering as that done using users' channel gain. Due to inappropriate ordering of users, based on distance, leads to degradation in users' outage performance. Similarly, in the scenario with no CSI feedback, random ordering of users is performed at the BS. Random ordering of the users translates to random power allocation. Hence, no CSI feedback results in degraded outage probability at the user. Utilizing the proposed FS for user ordering ensures that users are ordered based on the feedback received by them regarding their channel gain. Based on the feedback, appropriate power is allocated to users, therefore, the proposed FS yields better outage performance. In agreement with (42), at high SNR, the outage probability of Gr-0 user using the proposed FS shows an error floor, therefore, verifying the analytical findings of Section V-E1.

Fig. 1(b) illustrates the outage probability for Gr-1 user at the sub-6 GHz-SBS tier. Similar to Fig. 1(a), the outage probability curves for Gr-1 user in Fig. 1(b) shows similar trend. One major difference in the outage probability for Gr-0 and Gr-1 user is that for Gr-0 user, worst performance is observed with UDI, while for Gr-1 user, worst performance is

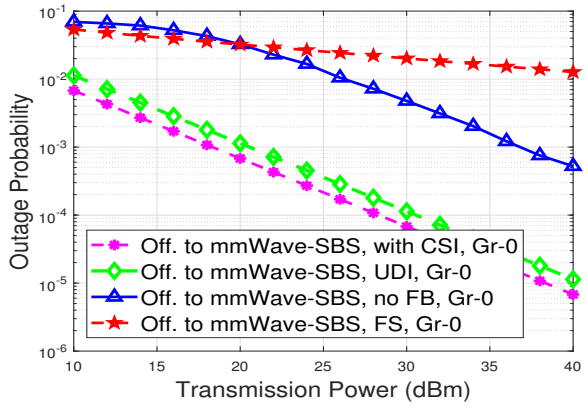

(a)

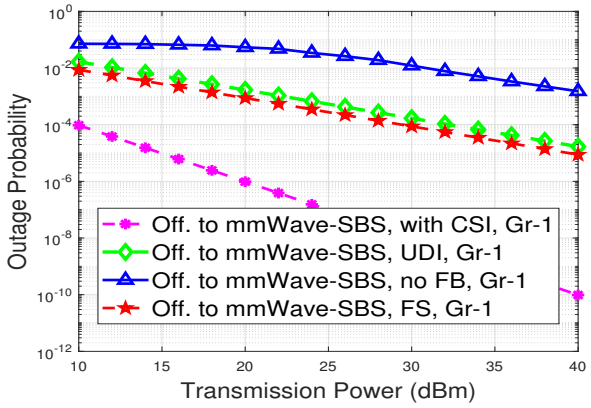

(b)

Fig. 4: Tier-outage probability at mmWave-SBS after offloading and RAT selection(a) For Gr-0 user. (b) For Gr-1 user.

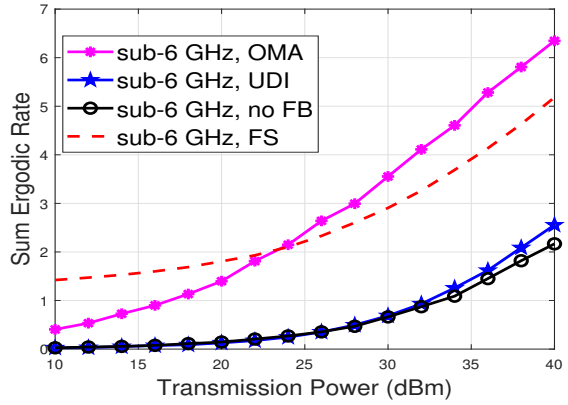

(a)

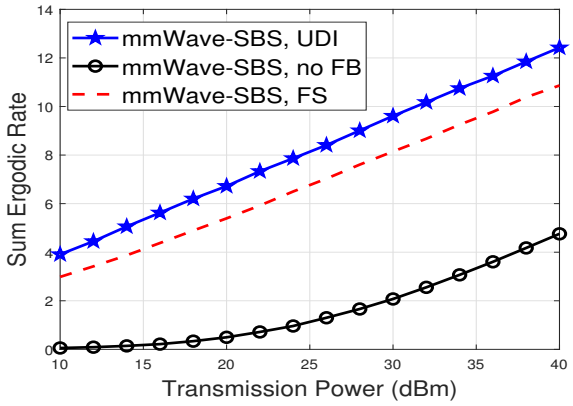

(b)

Fig. 6: Sum ergodic rate at sub-6 GHz-SBS and mmWave-SBS tier using partial CSI. (a) At sub-6 GHz-SBS tier. (b) At mmWave-SBS tier.

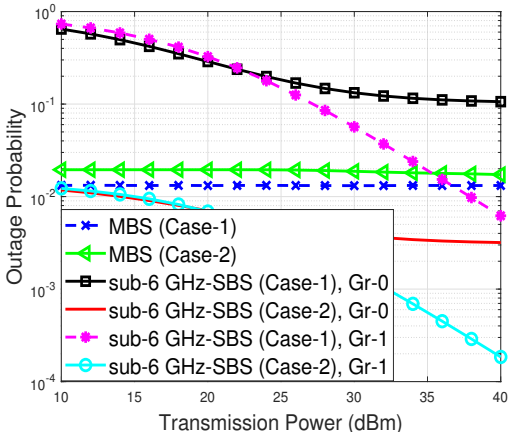

Fig. 5: Comparison of NOMA enabled multi-RAT HetNet (i.e., proposed NOMA-HHN) with NOMA enabled single-RAT HetNet

shown under no feedback scenario. The reason for Gr-1 user showing degraded performance with no feedback as compared to Gr-0 user is due to the random ordering of the users. Due to the random ordering, Gr-0 user may be considered to be Gr-1 user instead. As per NOMA principle, lower power is allocated to the Gr-1 user. Due to lower power allocation, performance of the selected Gr-1 user degrades, since the selected Gr-1 user might be a Gr-0 user which has been allocated less power.

Fig. 2(a) and Fig. 2(b) demonstrate the outage probability for Gr-0 user and Gr-1 user of the mmWave-SBS tier, respectively. It is interesting to note that for Gr-0 user of the mmWave-SBS tier, similar to the sub-6 GHz-SBS tier, perfect CSI achieves best outage performance. However, outage probability with no feedback and with UDI does not follow similar trends as that of the sub-6 GHz-SBS tier. For the mmWave-SBS tier, coverage range of the BS is very small as compared to that of the sub-6 GHz-SBS. Therefore, UDI can be considered as a nearly accurate measure of the users' actual channel condition. Hence, with UDI at the mmWave-SBS, the outage performance achieved at Gr-0 user is nearly same as that achieved by using perfect CSI. Furthermore, as explained for the sub-6 GHz-SBS tier, unavailability of feedback from users yield better performance for Gr-0 user as compared to that for Gr-1 user. The reason is similar to that explained for the sub-6 GHz-SBS tier. The selected Gr-0 user, which apparently is a Gr-1 user, is allocated higher power. The combination of good channel condition and more power results in improved performance at the selected Gr-

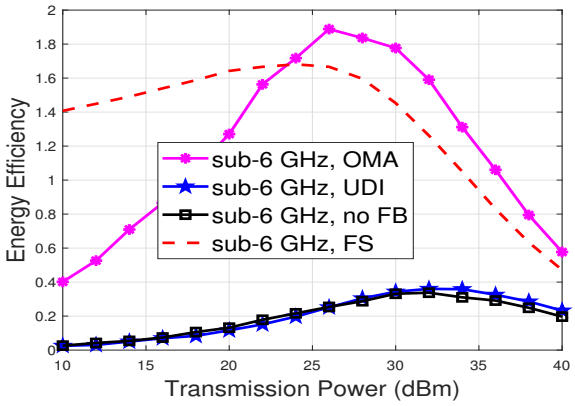

(a)

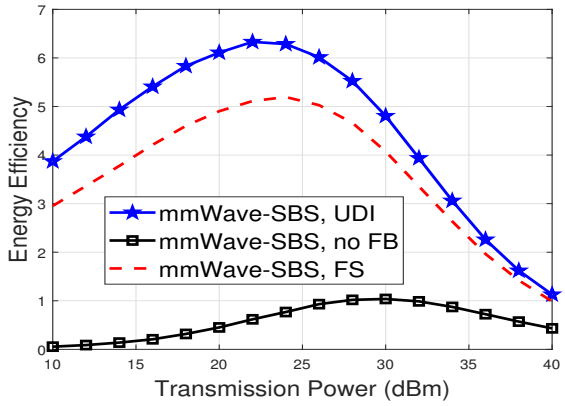

(b)

Fig. 7: Energy efficiency at sub-6 GHz-SBS and mmWave-SBS tier using partial CSI. (a) At sub-6 GHz-SBS tier. (b) At mmWave-SBS tier.

0 user. However, the condition reverses for the selected Gr-1 user, thereby resulting in degraded outage performance. Therefore, as can be observed from Fig. 2(b), the scenario with no feedback from the users achieves worst performance for the randomly selected Gr-1 user.

Fig. 3 and Fig. 4 reveal the total outage probability at the sub-6 GHz-SBS tier and mmWave-SBS tier, respectively, after offloading and RAT selection. It can be noted that Fig. 3(a), (b) and Fig. 4(a), (b), follow similar trend in outage probability similar to their counterparts in Fig. 1(a), (b), and Fig. 2(c), (d), respectively. However, it must be noted that when offloading is not performed and user is allowed to connect only with the MBS tier, without any choice of offloading to other SBS tier and/or other RAT, the outage probability shows poor performance. For the selected parameters, the maximum improvement that can be achieved using offloading to sub-6 GHz tier is by 93.57% when offloaded as Gr-0 user and by 99.12% when offloaded as Gr-1 user. When offloading and RAT selection are performed, regardless of whether or not CSI is known at the BS, the user's outage performance improves considerably. Besides, it is seen that offloading to the mmWave-SBS experiences significant improvement in outage probability as compared to without offloading and offloading to sub-6 GHz-SBS tier. The maximum improvement attained from offloading to mmWave-SBS tier is equivalent to nearly two times reduction in the outage probability before offloading. This justifies the requirement of HetNets with multi-RAT BSs for fulfilling the demands of future generation networks.

Fig. 5 shows the comparison between NOMA enabled HetNets using two competing technologies, namely, single-RAT network (hereafter referred to as Case-I) and multi-RAT network. The NOMA enabled HetNet utilizing multi-RAT network constitutes the proposed model (termed as (Case-II)). To maintain a fair comparison, while using single-RAT network, the power at the SBS is selected such that it equals the sum power of the sub-6 GHz-SBS and mmWave-SBS of the multi-RAT network, i.e., $P_s + P_m$. It is evident from Fig. 5 that Case-I yields improved outage probability at the MBS tier. This is due to the increased offloading probability from SBS to MBS tier as a result of increased SBS power (P_s to $P_s + P_m$). The increase in offloading probability with increased power is evident from (5) and implies more number of users being shifted to the sub-6 GHz tier. This effectively improves the outage probability at the MBS tier by 30.10%. However, if the outage probability at the sub-6 GHz tier is observed, it can be noted that Case-II yields much better performance as compared to Case-I. The improvement in outage probability at sub-6 GHz tier achieved by using Case-II is 97.09% for Gr-0 user and 97.24% for Gr-1 user. The reason for the degradation of outage probability at sub-6 GHz tier in Case-I is higher power at the sub-6 GHz which increases the co-tier interference at the user leading to increase in outage probability [31]. Therefore, single-RAT networks with incremental changes, e.g., power, will not suffice the growing demand and users. New techniques and wider bandwidths are essential for the future generation networks.

A. Ergodic Rate Calculation

The ergodic rate at the n^{th} user is evaluated as

$$\mathcal{E}_n = \mathbb{E}\left[1 + \log(\gamma_n)\right], \tag{48}$$

where γ_n denotes SINR at the n^{th} user of the considered tier. The sum ergodic rate for the proposed NOMA-HHN is computed by adding the ergodic rate of all the users served by the BS using NOMA and can be expressed as $\mathcal{E}_{sum} = \sum_{n=1}^{N} \mathcal{E}_n$. Fig. 6(a), and (b) show plots for the sum ergodic rate at the sub-6 GHz-SBS tier and mmWave-SBS tier using different types of partial CSI. It is evident from Fig. 6(a) that the sum ergodic rate achieved at the sub-6 GHz-SBS tier using NOMA is best and is nearly 4.3 times higher when the proposed FS is utilized as compared to with no feedback scenario and with UDI. The reason for achieving degraded performance using no feedback, and with UDI is the incorrect ordering of the users due to the unavailability of data and inaccurate data, respectively. The sum ergodic rate shows nearly the same performance in case of no feedback from users and with UDI. Moreover, it can be noticed that while using OMA at the sub-6 GHz-SBS tier, at low power, NOMA yields better performance. As the power is increased beyond 24dBm, the sum ergodic rate of OMA surpasses that of NOMA. The

reason is the increased interference at Gr-0 user from the message of Gr-1 user in the superimposed signal transmitted by the BS. Since, Gr-0 user does not perform SIC, hence the increased interference from Gr-1 user degrades the ergodic rate of Gr-0 user, which in turn reduces the sum ergodic rate at the sub-6 GHz-SBS tier at high SNR. However, from the subsequent results in Fig. 7(a), and (b), it is observed that the optimum/maximum power to attain maximum EE for the sub-6 GHz-SBS tier and mmWave-SBS tier is lower for NOMA as compared to that required using OMA to achieve similar results. It is interesting to note that for the sub-6 GHz-SBS tier, the maximum power required with the proposed FS is 24dBm, as determined from Fig. 7(a). This power is the value from where the performance of OMA surpasses that of NOMA, rendering the gain achieved by OMA to be trivial. Fig. 6(b) reveals the sum ergodic rate at the mmWave-SBS tier under different CSI conditions. It can be noted that for the mmWave-SBS tier, the scenario with UDI yields the highest sum ergodic rate. The sum ergodic rate achieved with UDI is higher by 17.96% when compared to the proposed FS and is nearly 4.6 times higher as compared to no feedback. The reason for UDI achieving the best performance is the smaller coverage range of mmWave-SBS which renders the distance information as an accurate measure of users' channel condition.

B. Energy Efficiency Calculation

Fig. 7 displays the EE curves for the sub-6 GHz-SBS tier and the mmWave-SBS tier. The EE is evaluated as

$$\mathcal{EE} = \frac{\mathcal{E}_{sum}}{P_t + P_c}, \tag{49}$$

where P_t is the transmit power at BS, and P_c represents the power consumption of the circuits [42]. It can be noted that for both the tiers, on increasing the power of the SBS, the EE increases and then observes a decrease with further increase in the power after a fixed value. The reason for decrease in EE after reaching a maximum point is credited to (49). The expression in (49) depicts the method of calculating EE. It can be seen that the power term is present in both, the numerator (in the SINR term while calculating ergodic rate) and the denominator. Initially on increasing the power, the sum ergodic rate, i.e., the sum of the ergodic rate of Gr-0 user and Gr-1 user increases. However, as the power is further increased, the advantage of rising power is nulled by the simultaneously increasing interference at the user. This implies that slope of the ergodic rate versus transmit rate plot decreases at higher transmit power. Hence, a drop in the EE is observed after reaching a maximum point. However, for the given parameters, the power corresponding to the maximum EE can be considered as the maximum allowable power at the BS under different partial CSI assumptions. For the sub-6 GHz-SBS tier, the value of maximum power achieved with the proposed FS is determined to be 24dBm from Fig. 7(a). Similarly, while using no feedback and with UDI the maximum power achieved is 32dBm. For sub-6 GHz-SBS using OMA with feedback, the maximum EE is achieved at a power of 26dBm. A similar analysis for Fig. 7(b) reveals that the power required to achieve maximum EE for the mmWave-SBS tier with UDI, with proposed FS and without feedback is 22dBm, 24dBm, and 30dBm, respectively.

VII. Conclusion

This paper investigates the co-existence of multi-RAT technologies in the future generation wireless network using the proposed NOMA-HHN. The performance of the proposed NOMA-HHN is examined under a realistic assumptions using different partial CSI cases. Furthermore, the results are compared with the conventional perfect CSI scenario. Load balancing in the proposed NOMA-HHN is performed using offloading among tiers and between RATs. The proposed FS with DA addresses the issues of initial access delay in the mmWave-SBS using beamtraining. The numerical results demonstrate the benefits of using the proposed NOMA-HHN to support immense load on the future wireless networks.

Acknowledgments

This work is supported in part by the R&D project under the Visvesvaraya PhD Scheme of Ministry of Electronics and Information Technology, Government of India, being implemented by Digital India Corporation (formerly Media Lab Asia), in part by DST-UKIERI (DST/INT/UK/P-129/2016 and DST-UKIERI-2016-17-0060), and in part by the third phase of technical education quality improvement program (referred to as TEQIP-III) of Ministry of Human Resource Development (MHRD), Government of India, under the Collaborative Research Scheme.

Appendix A
Proof of Proposition 1

Assuming that the distance information is available at the sub-6 GHz-SBS, and the users are ordered based on their distance as $r_1^s \leq r_2^s \leq \cdots \leq r_n^s$, where r_n^s denotes the distance of n^{th} nearest user. The total channel gain is given by the combination of small scale Rayleigh fading and large scale path loss and is expressed as $|\tilde{h}_n^s|^2 = |\hat{h}_n^s|^2 (r_n^s)^{-\nu_s}$. The small-scale fading, $|\hat{h}_n^s|^2$ only weakly changes the large scale path loss $(r_n^s)^{-\nu_s}$, which motivates ordering based on distance [21]. It is important to note that the total channel gain might not have the same order as that of the distance. Next, we calculate CDF of the channel gain when only distance information is known at the sub-6 GHz-SBS. Assuming, the locations of the users are uniformly distributed within the disc of radius $\mathcal{Y}_s$ around the sub-6 GHz-SBS, the distance r_n^s from an arbitrary user to the sub-6 GHz-SBS has the PDF as

$$f_{r_n^s}(r) = \frac{2r}{\mathcal{Y}_s^2}, \tag{50}$$

Therefore, the CDF may be expressed as

$$F_{r_n^s}(r) = \frac{r^2}{\mathcal{Y}_s^2}, 0 < r \leq \mathcal{Y}_s. \tag{51}$$

Since $r_1^s \leq r_2^s \leq \cdots \leq r_N^s$, by applying order statistics [43], PDF of Euclidean distance r_n^s is calculated as follows

$$f^d_{r^s_n}(r) = k\binom{N}{n}(F_{r^s_n}(r))^{n-1}(1-F_{r^s_n}(r))^{N-n} f_{r^s_n}(r) = 2n\binom{N}{n}\sum_{j=0}^{N-n}\binom{N-n}{j}(-1)^j \frac{r^{2(n+j)-1}}{{\mathcal{Y}_s}^{2(n+j)}}. \quad (52)$$

The CDF of the channel gain can be evaluated as

$$F^d_{|h^s_n|^2}(z) = \mathcal{P}\left\{\frac{|h^s_n|^2}{(r^s_n)^{\nu_s}} \le z\right\} = \int_0^{\mathcal{Y}_s}(1-e^{-z(r^s_n)^{\nu_s}}) f^d_{r^s_n}(r)dr. \quad (53)$$

The outage probability with UDI can be expressed as $\mathcal{O}^{s,d}_n = F^d_{|h^s_n|^2}(y^{s,d}_n)$, where $y^{s,d}_n = \epsilon^s_{max}(1+\sum_t \rho^I_t \mathcal{I}_t)$.

Appendix B
Proof of Proposition 2

Using the condition to be a Gr-0 user (as explained in Section III-B), the CDF of the channel for a user in Gr-0 can be evaluated as

$$F^{s,f}_0(y) = \frac{\mathcal{P}\left(|\tilde{h}^s_n|^2 < \min\{y,\zeta_s\}\right)}{\mathcal{P}\left(|\tilde{h}^s_n|^2 < \zeta_s\right)} = \frac{F_{|\tilde{h}^s_n|^2}(\min\{y,\zeta_s\})}{F_{|\tilde{h}^s_n|^2}(\zeta_s)}. \quad (54)$$

The outage probability of a user in Gr-0 can be written as $\mathcal{O}^{s,f}_0 = \mathcal{P}\left(\log(1+\gamma^s_0) \ge R\right) = F^{s,f}_0(y^{s,f}_0)$, where $y^{s,f}_0 = \epsilon^s_1(1+\sum_t \rho^I_t \mathcal{I}_t)$. Using (17) and (54), the outage probability for $\zeta_s < y^{s,f}_0$ is always equal to 1 while for $\zeta_s > y^{s,f}_0$ is evaluated as

$$\mathcal{O}^{s,f}_0 = \sum_{z=0}^{Z} b^s_z e^{-s^s_0}\mathcal{L}_{\mathcal{I}_s}(s^s_0\rho^I_s)\mathcal{L}_{\mathcal{I}_c}(s^s_0\rho^I_c)/\sum_{z=0}^{Z} b^s_z e^{-c^s_z\zeta_s}, \quad (55)$$

where $s^s_0 = c^s_z\epsilon^s_1$. Again, using the condition to be a Gr-1 user (as explained in Section III-B), the CDF of the channel gain for a user in Gr-1 is expressed as

$$F^{s,f}_1(y) = \frac{\mathcal{P}\left(\zeta_s < |\tilde{h}^s_n|^2 < y\right)}{\mathcal{P}\left(|\tilde{h}^s_n|^2 > \zeta_s\right)} = \frac{F_{|\tilde{h}^s_n|^2}(y) - F_{|\tilde{h}^s_n|^2}(\zeta_s)}{1-F_{|\tilde{h}^s_n|^2}(\zeta_s)}, \quad (56)$$

if $y > \zeta_s$, otherwise $F^{s,f}_1(y) = 0$. Similarly, for user in Gr-1, the outage probability can be calculated as

$$\mathcal{O}^{s,f}_1 = 1-\mathcal{P}\left(\log(1+\gamma^s_{1\to 0}) \ge R, \log(1+\gamma^s_1) \ge R\right) = F^{s,f}_1(y^{s,f}_1), \quad (57)$$

where $y^{s,f}_1 = \epsilon^s_{max}(1+\sum_t \rho^I_t \mathcal{I}_t)$. Therefore, the outage probability is given as

$$\mathcal{O}^{s,f}_1 = \sum_{z=0}^{Z} b_z e^{-s^s_1}\mathcal{L}_{\mathcal{I}_s}(s^s_1\rho^I_s)\mathcal{L}_{\mathcal{I}_c}(s^s_1\rho^I_c) - \mathcal{X}/(1-\mathcal{X}), \quad (58)$$

where $\mathcal{X} = \sum_{z=0}^{Z} b_z e^{-c^s_z\zeta_s}$ and $s^s_1 = c^s_z\epsilon^s_{max}$.

Appendix C
Proof of Proposition 3

Assuming that the distance information is available at the mmWave-SBS, and the users on the beam be ordered based on their distance as $r^m_1 \le r^m_2 \le \cdots \le r^m_N$, where r^m_n denotes the distance of the n^{th} nearest user. The total channel gain is given by the combination of small scale Rayleigh fading and large scale path loss and is expressed as $|\tilde{\mathbf{h}}^*_n|^2 = |\tilde{\mathbf{h}}^{**}_n|^2 (r^m_n)^{-\nu_m}$, where $|\tilde{\mathbf{h}}^{**}_n|^2 = |\hat{h}^m_n|^2 \frac{\sin^2\left(\frac{\pi M(\theta-\theta_n)}{2}\right)}{M\sin^2\left(\frac{\pi(\theta-\theta_n)}{2}\right)} = |\hat{h}^m_n|^2 F_M(\pi[\theta-\theta_n])$. Next, we calculate the CDF of the ordered channel gain when only distance information is known at the mmWave-SBS. Similar to sub-6 GHz-SBS, assuming the locations of the users to be uniformly distributed within the disc of radius $\mathcal{Y}_m$ around the mmWave-SBS, the distance r^m_n from an arbitrary user to the mmWave-SBS will follow the PDF and CDF as $f_{r^m_n}(r) = \frac{2r}{\mathcal{Y}^2_m}$ and $F_{r^m_n}(r) = \frac{r^2}{\mathcal{Y}^2_m}, 0 < r \le \mathcal{Y}_m$, respectively.

Hence, PDF of Euclidean distance r^m_n of the n^{th} nearest user can be expressed as

$$f^d_{r^m_n}(r) = k\binom{N}{n}(F_{r^m_n}(r))^{n-1}(1-F_{r^m_n}(r))^{N-n} f_{r^m_n}(r) = 2n\binom{N}{n}\sum_{j=0}^{N-n}\binom{N-n}{j}(-1)^j \frac{r^{2(n+j)-1}}{{\mathcal{Y}_m}^{2(n+j)}}. \quad (59)$$

The CDF of the channel gain $|\mathbf{h}^*_n|^2$ can be evaluated as

$$F^d_{|\mathbf{h}^*_n|^2}(z) = \mathcal{P}\left\{\frac{|\tilde{\mathbf{h}}^{**}_n|^2}{(r^m_n)^{\nu_m}} \le z\right\}, = \int_0^{\mathcal{Y}_m}(1-e^{\frac{-zr^{\nu_m}}{F_M}}) f^d_{r^m_n}(r)dr, \quad (60)$$

For n^{th} user, the outage probability can be determined using the SINR in (12) and (13) as

$$\mathcal{O}^{m,d}_n = 1-\mathcal{P}\left(\gamma^m_{n\to j} > R, \gamma^m_n > R\right) \quad (61)$$

Thus, the outage probability with UDI may be expressed as $\mathcal{O}^{m,d}_n = F^d_{|\mathbf{h}^*_n|^2}(y^{m,d}_n)$, where $y^{m,d}_n = \epsilon^m_{max}$.

Appendix D
Proof of Proposition 4

Similar to (54), the CDF of the channel gain of a user for $\zeta_m > 0$, if it lies in Gr-0 at the mmWave-SBS is expressed as

$$F^{m,f}_0(y) = \frac{\mathcal{P}\left(|\tilde{\mathbf{h}}^*_n|^2 < \min\{y,\zeta_m\}\right)}{\mathcal{P}\left(|\tilde{\mathbf{h}}^*_n|^2 < \zeta_m\right)} = \frac{F_{|\tilde{\mathbf{h}}^*_n|^2}(\min\{y,\zeta_m\})}{F_{|\tilde{\mathbf{h}}^*_n|^2}(\zeta_m)}. \quad (62)$$

The outage probability of user in Gr-0 can be expressed as

$$\mathcal{O}^{m,f}_0 = \mathcal{P}\left(\log(1+\gamma^m_1) \le R\right) = F^{m,f}_0(y^{m,f}_0), \quad (63)$$

where $y^{m,f}_0 = \epsilon^m_1$. Similarly, if $y > \zeta_m$, the CDF of the effective channel gain for user in Gr-1 can be expressed as

$$F^{m,f}_1(y) = \frac{\mathcal{P}\left(\zeta_m < |\tilde{\mathbf{h}}^*_n|^2 < y\right)}{\mathcal{P}\left(|\tilde{\mathbf{h}}^*_n|^2 > \zeta_m\right)} = \frac{F_{|\tilde{\mathbf{h}}^*_n|^2}(y) - F_{|\tilde{\mathbf{h}}^*_n|^2}(\zeta_m)}{1-F_{|\tilde{\mathbf{h}}^*_n|^2}(\zeta_m)}. \quad (64)$$

For $y < \zeta_m$, $F^{m,f}_1(y) = 0$. For user in Gr-1, the outage probability can be determined as

$$\mathcal{O}^{m,f}_1 = 1-\mathcal{P}\left(\log(1+\gamma^m_{2\to 1}) \ge R, \log(1+\gamma^m_2) \ge R\right). \quad (65)$$

This gives $\mathcal{O}^{m,f}_1 = F^{m,f}_1(y^{m,f}_1)$, where $y^{m,f}_1 = \epsilon^m_{max}$.

References

[1] H. S. Dhillon, R. K. Ganti, F. Baccelli, and J. G. Andrews, "Modeling and analysis of k-tier downlink heterogeneous cellular networks," *IEEE J. Sel. Areas Commu.*, vol. 30, no. 3, pp. 550–560, 2012.

[2] H.-S. Jo, Y. J. Sang, P. Xia, and J. G. Andrews, "Heterogeneous cellular networks with flexible cell association: A comprehensive downlink SINR analysis," *IEEE Trans. Wireless Commun.*, vol. 11, no. 10, pp. 3484–3495, 2012.

[3] J. G. Andrews, T. Bai, M. N. Kulkarni, A. Alkhateeb, A. K. Gupta, and R. W. Heath, "Modeling and analyzing millimeter wave cellular systems," *IEEE Trans. Commun.*, vol. 65, no. 1, pp. 403–430, 2017.

[4] T. Bai and R. W. Heath, "Coverage and rate analysis for millimeter-wave cellular networks," *IEEE Trans. Wireless Commun.*, vol. 14, no. 2, pp. 1100–1114, 2015.

[5] P. Swami, M. K. Mishra, V. Bhatia, and T. Ratnarajah, "Outage probability of ultra high frequency and millimeter wave based HetNets with NOMA," in *IEEE Int. Symposium Wireless Commun. Syst. (ISWCS)*, 2019, pp. 166–170.

[6] Z. Shi, W. Gao, S. Zhang, J. Liu, and N. Kato, "Machine learning-enabled cooperative spectrum sensing for non-orthogonal multiple access," *IEEE Trans. Wireless Commun.*, vol. 19, no. 9, pp. 5692–5702, 2020.

[7] J. Liu, Z. Shi, S. Zhang, and N. Kato, "Distributed Q-learning aided uplink grant-free NOMA for massive machine-type communications," *IEEE J. Sel. Areas Commun.*, vol. 39, no. 7, pp. 2029–2041, 2021.

[8] T.-H. Vu, T.-V. Nguyen, and S. Kim, "Cooperative NOMA-enabled SWIPT IoT networks with imperfect SIC: Performance analysis and deep learning evaluation," *IEEE Internet of Things Journal*, 2021.

[9] T.-H. Vu, T.-V. Nguyen, T.-T. Nguyen, and S. Kim, "Performance Analysis and Deep Learning Design of Wireless Powered Cognitive NOMA IoT Short-Packet Communications with Imperfect CSI and SIC," *IEEE Internet Things J.*, 2021.

[10] A. Damnjanovic, J. Montojo, Y. Wei, T. Ji, T. Luo, M. Vajapeyam, T. Yoo, O. Song, and D. Malladi, "A survey on 3GPP heterogeneous networks," *IEEE Wireless Commun.*, vol. 18, no. 3, 2011.

[11] J. Meredith, "Study on channel model for frequency spectrum above 6 GHz," 3GPP TR 38.900, Jun, Tech. Rep., 2016.

[12] Y. Li, J. G. Andrews, F. Baccelli, T. D. Novlan, and J. Zhang, "On the initial access design in millimeter wave cellular networks," in *IEEE Globecom Workshops (GC Wkshps)*, 2016, pp. 1–6.

[13] G. Ghatak, A. De Domenico, and M. Coupechoux, "Coverage analysis and load balancing in HetNets with millimeter wave multi-RAT small cells," *IEEE Trans. Wireless Commun.*, vol. 17, no. 5, pp. 3154–3169, 2018.

[14] Z. Pi and F. Khan, "An introduction to millimeter-wave mobile broadband systems," *IEEE Commun. Mag.*, vol. 49, no. 6, pp. 101–107, 2011.

[15] M. K. Mishra and A. Trivedi, "Spectral Efficiency and Deployment Cost Efficiency Analysis of mmW/UHF-Based Cellular Network," *IEEE Trans. Veh. Technol.*, vol. 68, no. 7, pp. 6565–6577, 2019.

[16] Z. Ding, X. Lei, G. K. Karagiannidis, R. Schober, J. Yuan, and V. K. Bhargava, "A survey on non-orthogonal multiple access for 5G networks: Research challenges and future trends," *IEEE J. Sel. Areas Commun.*, vol. 35, no. 10, pp. 2181–2195, 2017.

[17] Z. Wei, J. Yuan, D. W. K. Ng, M. Elkashlan, and Z. Ding, "A survey of downlink non-orthogonal multiple access for 5G wireless communication networks," *arXiv preprint arXiv:1609.01856*, 2016.

[18] M. Vaezi, G. A. A. Baduge, Y. Liu, A. Arafa, F. Fang, and Z. Ding, "Interplay between NOMA and other emerging technologies: A survey," *IEEE Trans. Cognitive Commun. Netw.*, vol. 5, no. 4, pp. 900–919, 2019.

[19] Y. Saito, Y. Kishiyama, A. Benjebbour, T. Nakamura, A. Li, and K. Higuchi, "Non-orthogonal multiple access (NOMA) for cellular future radio access," in *IEEE Veh. Technol. Conf. (VTC Spring)*, 2013, pp. 1–5.

[20] L. Dai, B. Wang, Y. Yuan, S. Han, I. Chih-Lin, and Z. Wang, "Non-orthogonal multiple access for 5G: solutions, challenges, opportunities, and future research trends," *IEEE Commun. Mag.*, vol. 53, no. 9, pp. 74–81, 2015.

[21] Z. Yang, Z. Ding, P. Fan, and G. K. Karagiannidis, "On the performance of non-orthogonal multiple access systems with partial channel information," *IEEE Trans. Commun.*, vol. 64, no. 2, pp. 654–667, 2015.

[22] Z. Ding, F. Adachi, and H. V. Poor, "The application of MIMO to non-orthogonal multiple access," *IEEE Trans. Wireless Commun.*, vol. 15, no. 1, pp. 537–552, 2016.

[23] Y. Liu, Z. Qin, M. Elkashlan, A. Nallanathan, and J. A. McCann, "Non-orthogonal multiple access in large-scale heterogeneous networks," *IEEE J. Sel. Areas Commun.*, vol. 35, no. 12, pp. 2667–2680, Dec 2017.

[24] Y. Liu, Z. Ding, M. Elkashlan, and H. V. Poor, "Cooperative non-orthogonal multiple access with simultaneous wireless information and power transfer," *IEEE J. Sel. Areas Commun.*, vol. 34, no. 4, pp. 938–953, 2016.

[25] Z. Ding, P. Fan, and H. V. Poor, "Random beamforming in millimeter-wave NOMA networks," *IEEE Access*, vol. 5, pp. 7667–7681, 2017.

[26] G. Lee, Y. Sung, and J. Seo, "Randomly-directional beamforming in millimeter-wave multiuser MISO downlink," *IEEE Trans. Wireless Commun.*, vol. 15, no. 2, pp. 1086–1100, 2016.

[27] B. Niu, O. Simeone, O. Somekh, and A. M. Haimovich, "Ergodic and outage performance of fading broadcast channels with 1-bit feedback," *IEEE Trans. Veh.Technol.*, vol. 59, no. 3, pp. 1282–1293, 2009.

[28] P. Xu, Y. Yuan, Z. Ding, X. Dai, and R. Schober, "On the outage performance of non-orthogonal multiple access with 1-bit feedback," *IEEE Trans. Wireless Commun.*, vol. 15, no. 10, pp. 6716–6730, 2016.

[29] S. N. Donthi and N. B. Mehta, "Joint performance analysis of channel quality indicator feedback schemes and frequency-domain scheduling for lte," *IEEE Transactions on Vehicular Technology*, vol. 60, no. 7, pp. 3096–3109, 2011.

[30] P. Swami, V. Bhatia, S. Vuppala, and T. Ratnarajah, "A cooperation scheme for user fairness and performance enhancement in NOMA-HCN," *IEEE Trans. Veh. Technol.*, vol. 67, no. 12, pp. 11 965–11 978, 2018.

[31] J. G. Andrews, F. Baccelli, and R. K. Ganti, "A tractable approach to coverage and rate in cellular networks," *IEEE Trans. Commun.*, vol. 59, no. 11, pp. 3122–3134, 2011.

[32] T. S. Rappaport, E. Ben-Dor, J. Murdock, and Y. Qiao, "38 GHz and 60 GHz angle-dependent propagation for cellular & peer-to-peer wireless communications." in *IEEE International Conf. Commun. (ICC)*, 2012, pp. 4568–4573.

[33] P. Swami, M. K. Mishra, V. Bhatia, and T. Ratnarajah, "Performance analysis of NOMA enabled hybrid network with limited feedback," *IEEE Trans. Veh. Technol.*, vol. 69, no. 4, pp. 4516–4521, 2020.

[34] S. Singh, H. S. Dhillon, and J. G. Andrews, "Offloading in heterogeneous networks: Modeling, analysis, and design insights," *IEEE Trans. Wireless Commun.*, vol. 12, no. 5, pp. 2484–2497, 2013.

[35] A. Kangas and T. Wigren, "Angle of arrival localization in LTE using MIMO pre-coder index feedback," *IEEE Commun. Lett.*, vol. 17, no. 8, pp. 1584–1587, 2013.

[36] H. Elshaer, M. N. Kulkarni, F. Boccardi, J. G. Andrews, and M. Dohler, "Downlink and uplink cell association with traditional macrocells and millimeter wave small cells," *IEEE Trans. Wireless Commun.*, vol. 15, no. 9, pp. 6244–6258, 2016.

[37] S. N. Chiu, D. Stoyan, W. S. Kendall, and J. Mecke, *Stochastic geometry and its applications*. John Wiley & Sons, 2013.

[38] Y. Liu, Z. Ding, M. Elkashlan, and J. Yuan, "Non-orthogonal multiple access in large-scale underlay cognitive radio networks," *IEEE Trans. Veh. Technol.*, vol. 65, no. 12, pp. 10 152–10 157, 2016.

[39] Z. Ding, Z. Yang, P. Fan, and H. V. Poor, "On the performance of non-orthogonal multiple access in 5G systems with randomly deployed users," *IEEE Signal Process. Lette.*, vol. 21, no. 12, pp. 1501–1505, 2014.

[40] J. Stoer and R. Bulirsch, *Introduction to numerical analysis*. Springer Sci. Business Media, 2013.

[41] J. Venkataraman, M. Haenggi, and O. Collins, "Shot noise models for outage and throughput analyses in wireless ad hoc networks," in *IEEE Military Commun. Conf. (MILCOM)*, 2006, pp. 1–7.

[42] J. B. Rao and A. O. Fapojuwo, "On the tradeoff between spectral efficiency and energy efficiency of homogeneous cellular networks with outage constraint," vol. 62, no. 4, pp. 1801–1814, 2012.

[43] H. A. David and H. N. Nagaraja, "Order statistics," *Encyclopedia of Statistical Sciences*, 2004.